

AZPH-TH/97-13
FSU-SCRI-97-130
IUHET-374
NORDITA-97/84P

Quenched hadron spectroscopy with improved staggered quark action

Claude Bernard

Department of Physics, Washington University, St. Louis, MO 63130, USA

Tom Blum

Department of Physics, Brookhaven National Lab, Upton, NY 11973, USA

Thomas A. DeGrand

Physics Department, University of Colorado, Boulder, CO 80309, USA

Carleton DeTar, Craig McNeile

Physics Department, University of Utah, Salt Lake City, UT 84112, USA

Steven Gottlieb

Department of Physics, Indiana University, Bloomington, IN 47405, USA

Urs M. Heller

SCRI, Florida State University, Tallahassee, FL 32306-4130, USA

James Hetrick

Physics Department, University of the Pacific, Stockton, CA 95211-0197, USA

K. Rummukainen

NORDITA, Blegdamsvej 17, DK-2100 Copenhagen Ø, Denmark

Bob Sugar

Department of Physics, University of California, Santa Barbara, CA 93106, USA

Doug Toussaint

Department of Physics, University of Arizona, Tucson, AZ 85721, USA

We investigate light hadron spectroscopy with an improved quenched staggered quark action. We compare the results obtained with an improved gauge plus an improved quark action, an improved gauge plus standard quark action, and the standard gauge plus standard quark action. Most of the improvement in the spectroscopy results is due to the improved gauge sector. However, the improved quark action substantially reduces violations of Lorentz invariance, as evidenced by the meson dispersion relations.

1 Introduction

The precision of numerical lattice QCD simulations with the standard lattice actions is constrained by the available computational resources. In order to keep the duration of the calculation within manageable bounds, one is forced to use lattice spacings a which may be too large to accurately describe the continuum physics. This problem has been addressed by the development of improved [1, 2, 3] and fixed-point [4, 5] actions. The promise of these actions is to yield good approximations to the continuum physics with relatively coarse lattice spacings. (For a recent review, see [6].)

In the Symanzik improvement scheme [1, 2] the lattice action and fields are improved in powers of the lattice spacing a . This is achieved by introducing higher dimensional terms into the action. In the continuum limit, these terms are irrelevant, but at a finite cutoff the coefficients of these terms can be tuned so that the discretization errors of spectral quantities are diminished. The most straightforward method to determine the coefficients is to expand the action in a Taylor series in a , and cancel the leading scaling violating terms order by order (tree-level improvement). This can be refined by using perturbative analysis or non-perturbative numerical methods to determine the coefficients.

In this paper, we study the improvement of the staggered (Kogut-Susskind) quark lattice QCD action with quenched spectroscopy calculations. The improvement is implemented by adding a third-nearest-neighbor term, first proposed by Naik more than a decade ago [7]. Some of the preliminary results of this study have already been published in [8, 9]. The same improvement scheme has been applied to nonzero temperature calculations by Karsch et al. [10]. The gauge configurations used in this study are generated with an $\mathcal{O}(a^2)$ one-loop and tadpole-improved gauge action [2, 3]. Since our main goal is to investigate the effects of the fermionic improvement, we compare the hadronic spectrum obtained with both the unimproved and improved fermion actions, using the same gauge configurations. An excellent baseline for the evaluation of the improvement is provided by our extensive standard (non-improved) quenched Kogut-Susskind hadron spectroscopy calculation [11].

As opposed to Wilson fermions, the improvement of the staggered action has attracted relatively little attention. This is partly due to the formal complexity of the staggered formulation, partly to the fact that the standard Wilson fermions have an error $\mathcal{O}(a)$,

whereas the staggered action is already accurate to this order. Nevertheless, the improvement of the staggered action is highly desirable: the staggered action has a $U(1)\times U(1)$ chiral symmetry, remnant of the full continuum $U(4)\times U(4)$ symmetry (for 4 quark flavors). This symmetry is restored in the continuum limit; however, for practical values of the lattice spacing a substantial flavor symmetry breaking remains. This is a lattice artifact, and it remains a major problem when one studies the restoration of the spontaneously broken chiral symmetry at finite temperature. Moreover, the very successful $\mathcal{O}(a^2)$ improvement of the pure gauge action makes it very natural to try to bring the quark action to the same accuracy.

This paper is organized as follows: in section 2 we discuss the improvement of both the gauge and the fermion actions and the properties of the free fermion actions. In section 3 we present the results of the simulations and the comparison of the different actions. In particular, we study (a) the m_N/m_ρ mass ratios at several fixed values of m_π/m_ρ as functions of the lattice spacing, (b) the Lorentz invariance of π and ρ meson states, and (c) the restoration of the flavor symmetry (as determined by the mass difference of the pseudo-Goldstone and non-Goldstone π mesons). Our conclusions are presented in section 4.

2 Improvement of the action

2.1 The gauge action

We generate gauge configurations with the tadpole-improved $SU(3)$ gauge action [2, 3, 12]:

$$S_G = \beta_{\text{pl}} \sum_{x;\mu<\nu} (1 - P_{\mu\nu}) + \beta_{\text{rt}} \sum_{x;\mu\neq\nu} (1 - R_{\mu\nu}) + \beta_{\text{pg}} \sum_{x;\mu<\nu<\sigma} (1 - C_{\mu\nu\sigma}) \quad (1)$$

where P is the standard plaquette in the μ, ν -plane, and R and C denote the real part of the trace of the ordered product of $SU(3)$ link matrices along 1×2 rectangles and $1 \times 1 \times 1$ paths, respectively:

$$P_{\mu\nu} = \frac{1}{3} \text{Re Tr} \left[\begin{array}{|c|} \hline \leftarrow \\ \hline \leftarrow \rightarrow \\ \hline \rightarrow \\ \hline \end{array} \right] \quad (2)$$

$$R_{\mu\nu} = \frac{1}{3} \text{Re Tr} \left[\begin{array}{|c|} \hline \leftarrow \rightarrow \\ \hline \leftarrow \rightarrow \\ \hline \vdots \\ \hline \leftarrow \rightarrow \\ \hline \end{array} \right] \quad (3)$$

$$C_{\mu\nu\sigma} = \frac{1}{3} \text{Re Tr} \left[\text{Diagram} \right] \quad (4)$$

In general, the improvement conditions do not uniquely specify the form of the action. For example, at tree-level, adding either the planar 6-link term or one of several 8-link terms to the standard action would cancel the $\mathcal{O}(a^2)$ errors. However, when the quantum corrections are calculated with the lattice perturbation theory, then at least two terms are required to cancel $\mathcal{O}(g^{2n}a^2)$ errors [2]. The terms in Eq. (1) provide the most compact form of the action.

Due to the UV divergence of the tadpole-type graphs in lattice perturbation theory, operators formally of order a^n in the expansion of the action are changed to order $a^{n-2m}g^{2m}$ by quantum effects, depending on the number of tadpole graph contributions to that particular term. (In the tadpole contributions $n \geq 2m$, *i. e.* tadpoles do not introduce additional UV-divergencies.) The contribution of the tadpole diagrams can be partially taken into account by absorbing them in the lattice coupling constants. This is commonly achieved by the definition of the ‘average gauge link’ from the plaquette, $u_0 \equiv \langle P \rangle^{1/4}$, which is strongly dominated by tadpoles, and by replacing $U_i(x) \rightarrow U_i(x)/u_0$ in every lattice operator [3, 12]. This corresponds to a redefinition of the lattice gauge coupling $g^2 \rightarrow g^2/u_0^4$.

With these ingredients, the coefficients of the action (1) are related by the 1-loop expressions [12]

$$\beta_{\text{rt}} = -\frac{\beta_{\text{pl}}}{20 u_0^2} (1 + 0.4805\alpha_s) \quad (5)$$

$$\beta_{\text{pg}} = -\frac{\beta_{\text{pl}}}{u_0^2} 0.03325\alpha_s \quad (6)$$

where the strong coupling constant is determined through the 1-loop relation

$$\alpha_s = -4 \log(u_0)/3.0684. \quad (7)$$

The leading errors of this action are of order $\mathcal{O}(a^2\alpha_s^2, a^4)$.

2.2 Tree-level improvement of the quark action

In this work, we study the following fermion action:

$$\begin{aligned}
S_N &= a^4 \sum_{x;\mu} \eta_\mu(x) \bar{\chi}(x) \frac{1}{2a} \left\{ c_1 \left[U_\mu(x) \chi(x + \mu) - U_\mu^\dagger(x - \mu) \chi(x - \mu) \right] \right. \\
&+ c_2 \left[U_\mu(x) U_\mu(x + \mu) U_\mu(x + 2\mu) \chi(x + 3\mu) \right. \\
&\quad \left. \left. - U_\mu^\dagger(x - \mu) U_\mu^\dagger(x - 2\mu) U_\mu^\dagger(x - 3\mu) \chi(x - 3\mu) \right] \right\} \\
&+ a^4 m_q \sum_x \bar{\chi}(x) \chi(x),
\end{aligned} \tag{8}$$

where the phase factor $\eta_\mu(x) = (-1)^{(x_0+x_1+\dots+x_{\mu-1})}$. The standard Kogut-Susskind (staggered) action is obtained with coefficients $c_1 = 1$ and $c_2 = 0$. At tree level, the action is $\mathcal{O}(a^2)$ accurate when $c_1 = 9/8$ and $c_2 = -1/24$. In this case, the *difference* from the Kogut-Susskind action is a discrete version of the 3rd order derivative:

$$\frac{1}{8} \frac{f(x + \hat{\mu}) - f(x - \hat{\mu})}{2a} - \frac{1}{24} \frac{f(x + 3\hat{\mu}) - f(x - 3\hat{\mu})}{2a} = -\frac{a^2}{6} \partial_\mu^3 f(x) + \mathcal{O}(a^4). \tag{9}$$

The staggered action with a third nearest neighbor term was originally proposed by Naik [7]. However, he was studying the improvement of the Dirac-Kähler action, which has a different coupling to the gauge fields than the action in Eq. (8). The Dirac-Kähler action lacks the exact $U(1) \times U(1)$ -symmetry enjoyed by the action (8), and the bare quark mass has to be additively renormalized. These properties make use of the Dirac-Kähler action much less appealing than the Kogut-Susskind action. Nevertheless, in the following we shall call the action (8) the Naik action.

The (one-component) Grassmann field χ describes 4 flavors of Dirac fermions in the continuum limit. This is not transparent in Eq. (8), nor can one easily identify the leading irrelevant terms when the continuum limit is taken. At the free fermion level, perhaps the easiest way to see this is to use the following transformation [13]: in momentum space, we decompose the momentum vector $k = p + \pi A/a$, $A_\mu = 0$ or 1 , and we restrict $0 \leq k < \pi/a$. A new (16-component) fermion field ψ is defined as

$$\psi(p) = \frac{1}{8} \sum_{A,B} (-1)^{A \cdot B} \Gamma_A \chi(p + \pi B/a) \tag{10}$$

$$\bar{\psi}(p) = \frac{1}{8} \sum_{A,B} (-1)^{A \cdot B} \Gamma_A^\dagger \bar{\chi}(p + \pi B/a). \tag{11}$$

where

$$\Gamma_A = \gamma_0^{A_0} \gamma_1^{A_1} \gamma_2^{A_2} \gamma_3^{A_3}. \quad (12)$$

In terms of field ψ , the free action (8) becomes

$$S_{\text{free}} = \sum_p \bar{\psi}(p) \left[\sum_\mu \gamma_\mu \frac{i}{a} (c_1 \sin p_\mu a + c_2 \sin 3p_\mu a) + m \right] \psi(p). \quad (13)$$

This form of the action is flavor diagonal; however, if we perform an inverse Fourier transform, the derivative term becomes nonlocal. The Kogut-Susskind action ($c_2 = 0$) has leading $\mathcal{O}(a^2)$ errors. The coefficients $c_1 = 9/8$ and $c_2 = -1/24$ for the Naik action are readily recovered from Eq. (13) by expanding the trigonometric functions.

When the gauge fields are included one cannot transform the action (8) to the form in Eq. (13). It is not at all obvious that the interacting Kogut-Susskind action is still $\mathcal{O}(a)$ -accurate. In order to see the flavor structure more clearly, one usually performs the (local) transformation originally proposed by Kluberg-Stern et al. [14]. It transforms the 1-component staggered field χ to a hypercubic 16-component ‘quark field’ (4 flavors of 4-component Dirac spinors), which lives on a lattice with twice the original lattice spacing. The quark field action cannot be written in a compact form, but when expanded in powers of the lattice spacing a it has apparent dimension-5 terms (giving rise to $\mathcal{O}(a)$ errors).

However, the Kogut-Susskind action does *not* have on-shell $\mathcal{O}(a)$ errors. This has been shown by Sharpe [15] and Luo [16, 17] by a generalization of the Kluberg-Stern et al. transformation. The leading scaling violations start at $\mathcal{O}(a^2)$. In order to cancel them, one has to add dimension-6 terms to the action; these terms have been classified by Luo [17]. The terms fall into two classes: $\bar{\psi} D^3 \psi$ terms, where D^3 is a generic combination of 3 covariant derivatives (and to which class the ‘Naik term’ in Eq. (8) belongs), and 4-fermion terms. Unfortunately, even in the simplest form, the action has 15 dimension-6 terms with — so far — unknown coefficients. Therefore, we limit ourselves here to a much more modest goal and study the degree of improvement possible to obtain with the action (8), bearing in mind that this action cannot cancel all of the $\mathcal{O}(a^2)$ errors, but only the ones present already for free fermions.

As with the gauge action, we may improve the action (8) beyond the tree-level by taking into account the modifications due to gluon tadpoles: with the replacement $U \rightarrow U/u_0$,

the coefficients c_i in action (8) become

$$c_1 = \frac{9}{8u_0} \quad c_2 = -\frac{1}{24u_0^3}. \quad (14)$$

In this work we use the quark action defined by Eqs. (8,14). In the nonzero temperature calculation in Ref. [10] the action (8) was used with the ‘tree-level’ values.

2.3 Properties of the free quark action

The free quark dispersion relation $E(\mathbf{p})$ can be found from Eq. (13), by solving for the poles of the Euclidean propagator and using the identification $E = \text{Re } ip_0$. In Fig. 1 we show the massless quark dispersion relations for the standard Kogut-Susskind and Naik actions. For comparison, we also show the Wilson fermion action dispersion relation. The Naik action follows the continuum dispersion relation $E = |\mathbf{p}|$ much better than the standard Kogut-Susskind action up to $|\mathbf{p}| \sim 1.8/a$, not to mention the Wilson action (with the Wilson parameter $r = 1$). Note that for massless free quarks both the Wilson and the Kogut-Susskind actions have $\mathcal{O}(a^2)$ leading errors. Due to the third nearest neighbor coupling in the imaginary time direction, unphysical *ghost* branches (with complex ip_0) appear in the dispersion relation. These states will become infinitely massive when $a \rightarrow 0$.

For free fermions, the thermal energy can be easily calculated from $E = T^2 \partial \log Z / \partial T$. In the imaginary time formalism, the temperature $T = 1/(N_T a)$, the inverse temporal extent of the lattice. Under the assumption that the free energy is proportional to the volume, the pressure is $P = T \partial \log Z / \partial V$. In Fig. 2 we show E/T^4 and P/T^4 for free Kogut-Susskind, Wilson and Naik fermions as functions of the inverse lattice spacing. Also shown are the results from the Bielefeld ‘P4’ staggered action [18]: like the Naik action, it contains a 3rd nearest neighbor coupling, but in this case the neighbors are coupled along L-shaped paths (the Naik $\bar{\psi}(x)U_\mu(x)U_\mu(x + \hat{\mu})U_\mu(x + 2\hat{\mu})\psi(x + 3\hat{\mu})$ -terms are replaced with terms of form $\bar{\psi}(x)U_\mu(x)U_\nu(x + \hat{\mu})U_\nu(x + \hat{\mu} + \hat{\nu})\psi(x + \hat{\mu} + 2\hat{\nu})$, with $\nu \neq \mu$). The P4 action yields the same tree-level improvement as the Naik action. (For a comparison with a renormalization group improved free staggered quark action, see the last paper of Ref. [5].)

The energy and pressure of the Naik fermions approach the continuum ideal fermion gas limits much faster than the standard Kogut-Susskind action. Indeed, the Bielefeld group

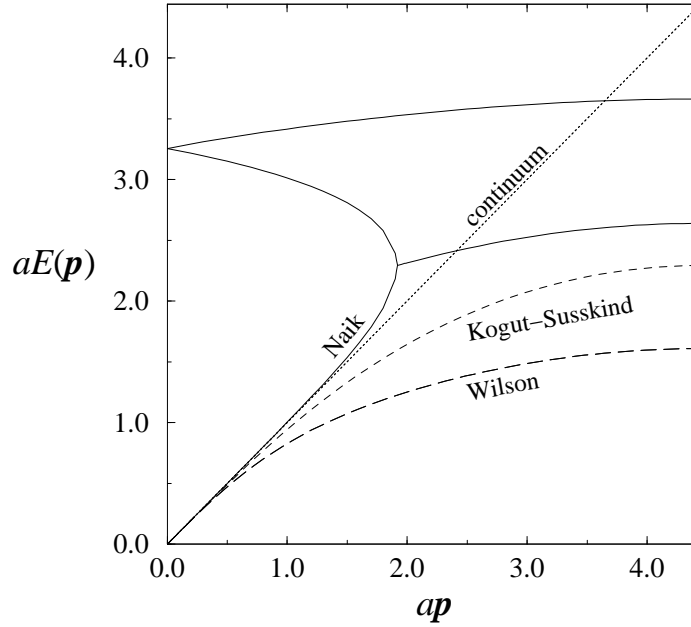


Figure 1: The dispersion relation $E(\mathbf{p})$ for massless free quarks with different fermion actions. The momentum \mathbf{p} is to the spatial direction $(1, 1, 0)$, and the dispersion relations are plotted up to the end of the Brillouin zone.

[10] reported an improved thermodynamic behavior even when the interacting gauge fields are included in a dynamical quark Monte Carlo simulation.

3 The simulations and the results

3.1 Hadron spectrum

The parameters of the action (1) used in the generation of the quenched configurations are shown in Table 1.

β_{pl}	u_0	volume	$N_{\text{conf.}}$
6.8	0.8261	$16^3 \times 32$	199
7.1	0.8441	$14^3 \times 28$	203
7.4	0.8629	$16^3 \times 32$	200
7.6	0.8736	$16^3 \times 32$	100
7.75	0.8800	$16^3 \times 32$	200
7.9	0.8848	$16^3 \times 32$	200

Table 1: The parameters of the runs. β_{rt} and β_{pg} can be obtained through Eqs. (5–7).

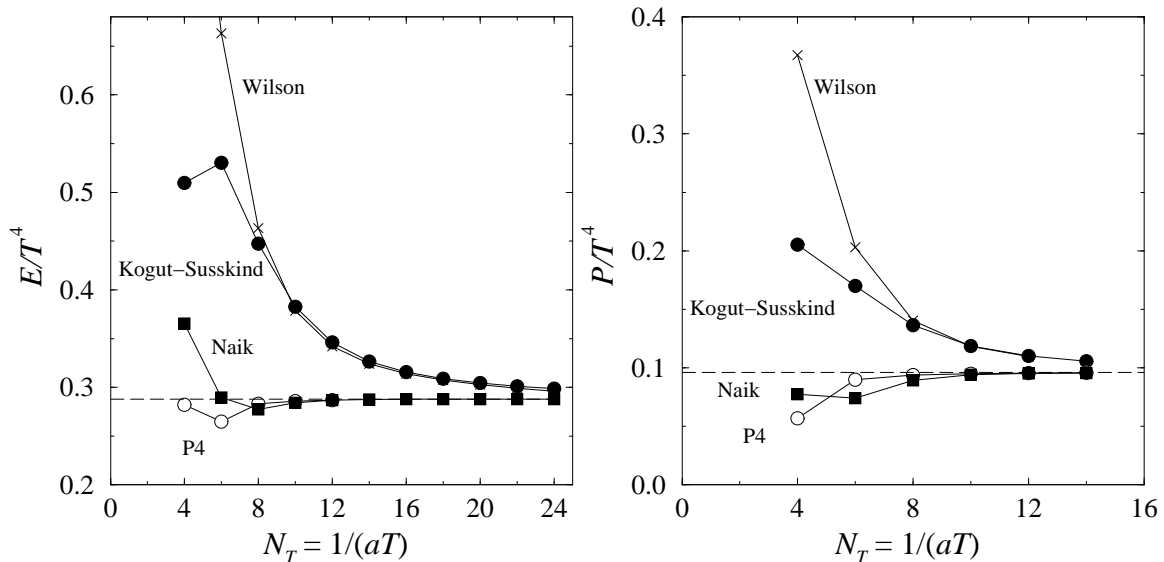


Figure 2: The energy (left) and the pressure (right) per fermion degree of freedom for free Kogut-Susskind, Naik, Wilson and “P4” [18] fermions as a function of $N_T = 1/(aT)$. The continuum values are shown with dashed lines.

We measure the masses of the nucleon, the Goldstone pion π , (corresponding to the (spontaneously broken) explicit U(1) chiral symmetry of the action (8)), the non-Goldstone (“SC”) pion π_2 , and the ρ and ρ_2 mesons. The masses were calculated both with the Naik and the Kogut-Susskind actions. For each lattice and propagator, we use four wall source planes. In each case, the hadron propagators were measured with 5–6 bare quark masses $am_q = 0.005 - 0.32$; the hadron masses are shown in Tables 2–4.

Throughout the analysis we quantify the performance of the improved actions by comparing the results against a non-improved benchmark — an extensive standard quenched Kogut-Susskind hadron spectroscopy study by the MILC collaboration [11]. In particular, we use $\beta_{\text{Wilson}} = 6/g^2 = 5.54$ (16^3), 5.7 (24^3), 5.85 (24^3) and 6.15 (32^3) lattices (with the spatial volume in parentheses).

The Naik hadron propagator calculation requires about 2 times more CPU time than the Kogut-Susskind one. The number of conjugate gradient iterations is very similar for the Naik and the Kogut-Susskind quarks, but since the Naik action (8) involves about twice as many terms, the computational load is higher. For example, for the $\beta_{\text{pl}} = 7.4$,

Naik, $\beta_{\text{pl}} = 6.8, 16^3 \times 32$

am_q	π	π_2	ρ	ρ_2	Nucleon
0.02	0.343438(70)	1.4(2)	1.537(15)	2.06(18)	2.301(50)
0.04	0.484458(64)	1.53(3)	1.617(24)	2.021(72)	2.387(19)
0.08	0.682699(82)	1.86(6)	1.6964(91)	2.098(29)	2.730(38)
0.16	0.962771(60)	2.12(3)	1.8581(75)	-	3.032(49)
0.32	1.365621(51)	-	2.061(27)	-	3.589(14)

Kogut-Susskind, $\beta_{\text{pl}} = 6.8, 16^3 \times 32$

am_q	π	π_2	ρ	ρ_2	Nucleon
0.02	0.350547(81)	1.411(75)	1.405(13)	1.73(13)	2.1632(93)
0.04	0.492871(80)	1.474(35)	1.4308(61)	1.642(48)	2.134(64)
0.08	0.689935(67)	1.524(16)	1.4816(25)	1.660(17)	2.3286(59)
0.16	0.959548(63)	1.640(10)	1.5772(37)	1.7389(56)	2.447(33)
0.32	1.325654(74)	1.8896(43)	1.75802(52)	1.9078(25)	2.7434(79)

Naik, $\beta_{\text{pl}} = 7.1, 14^3 \times 28$

am_q	π	π_2	ρ	ρ_2	Nucleon
0.02	0.35637(12)	1.289(39)	1.573(44)	1.595(67)	2.16(13)
0.04	0.50074(20)	1.473(59)	1.568(18)	1.651(38)	2.342(51)
0.08	0.70269(17)	1.585(26)	1.6188(70)	1.822(23)	2.459(31)
0.16	0.985219(93)	1.968(65)	1.822(12)	2.0087(83)	2.759(19)
0.32	1.389359(81)	2.874(80)	2.1188(39)	2.72(16)	3.384(74)

Kogut-Susskind, $\beta_{\text{pl}} = 7.1, 14^3 \times 28$

am_q	π	π_2	ρ	ρ_2	Nucleon
0.02	0.36368(13)	1.411(77)	1.338(14)	1.376(31)	1.990(37)
0.04	0.50958(13)	1.356(32)	1.403(18)	1.443(16)	2.190(59)
0.08	0.70934(13)	1.361(25)	1.4481(69)	1.5301(72)	2.278(18)
0.16	0.97939(11)	1.592(17)	1.5680(76)	1.6681(53)	2.414(11)
0.32	1.34259(10)	1.8213(89)	1.7423(15)	1.8574(16)	2.7142(25)

Table 2: Masses for $\beta_{\text{pl}} = 6.8, 16^3 \times 32$, and $\beta_{\text{pl}} = 7.1, 14^3 \times 28$ lattices. Entry ‘-’ means no good mass fits were possible.

$16^3 \times 32$ lattices the number of the conjugate gradient iterations for each source plane varies approximately from 130 ($am_q = 0.32$) to 2050 ($am_q = 0.02$) for the Kogut-Susskind and from 140 to 2400 for the Naik action, whereas the CPU time per plane for $am_q = 0.02$ is about 260 seconds for K-S and 600 seconds for Naik on the Intel Paragon using 32 nodes.

In order to find the best confidence levels of the propagator fits, we used one-, two- and three-particle fitting functions, varying both the beginning and the end of the fitting range.

Naik, $\beta_{\text{pl}} = 7.4, 16^3 \times 32$

am_q	π	π_2	ρ	ρ_2	Nucleon
0.02	0.37314(79)	1.033(30)	1.268(13)	1.294(34)	1.765(30)
0.04	0.52238(70)	1.0834(96)	1.3139(89)	1.383(14)	1.920(15)
0.08	0.72475(95)	1.2517(75)	1.4283(99)	1.5035(71)	2.1320(68)
0.16	1.0080(11)	1.5591(97)	1.6241(48)	1.768(14)	2.547(14)
0.32	1.416801(79)	2.146(23)	1.9719(25)	2.2396(79)	3.1459(76)

Kogut-Susskind, $\beta_{\text{pl}} = 7.4, 16^3 \times 32$

am_q	π	π_2	ρ	ρ_2	Nucleon
0.02	0.38080(74)	0.9603(66)	1.207(14)	1.247(33)	1.724(29)
0.04	0.5280(12)	1.0418(45)	1.2449(63)	1.337(43)	1.855(13)
0.08	0.7297(10)	1.1905(66)	1.3270(28)	1.4074(63)	2.0282(53)
0.16	0.9994(11)	1.4197(28)	1.4774(25)	1.5725(50)	2.3174(56)
0.32	1.362520(74)	1.7300(16)	1.69637(81)	1.7975(31)	2.6656(35)

Naik, $\beta_{\text{pl}} = 7.6, 16^3 \times 32$

am_q	π	π_2	ρ	ρ_2	Nucleon
0.01	0.27294(23)	-	0.945(28)	-	1.36(15)
0.02	0.38154(24)	0.7513(89)	1.0106(87)	1.046(11)	1.411(52)
0.04	0.53125(25)	0.8629(46)	1.0911(56)	1.1424(73)	1.598(11)
0.08	0.73613(23)	1.0559(32)	1.2420(53)	1.312(11)	1.852(40)
0.16	1.01922(24)	1.3667(35)	1.4682(31)	1.5441(56)	2.256(15)
0.32	1.42502(16)	1.9038(93)	1.8670(34)	2.0072(69)	2.9137(61)

Kogut-Susskind, $\beta_{\text{pl}} = 7.6, 16^3 \times 32$

am_q	π	π_2	ρ	ρ_2	Nucleon
0.01	0.28090(23)	-	0.945(29)	-	1.28(14)
0.02	0.39165(22)	0.7508(90)	0.9943(86)	1.031(11)	1.377(54)
0.04	0.54237(23)	0.8642(48)	1.0621(48)	1.190(15)	1.577(10)
0.08	0.74470(22)	1.0462(31)	1.2030(44)	1.2705(91)	1.804(33)
0.16	1.01321(19)	1.3092(27)	1.3882(22)	1.4474(38)	2.187(20)
0.32	1.36891(12)	1.6677(32)	1.6573(10)	1.7287(19)	2.5975(52)

Table 3: Masses for $\beta_{\text{pl}} = 7.4, 14^3 \times 28$, and $\beta_{\text{pl}} = 7.6, 16^3 \times 32$ lattices.

All of the fits use the full invariance matrix of the propagators. We block together all of the propagators on each lattice, then, in order to facilitate further analysis, we calculate the masses using a single elimination jackknife procedure. When fitting each jackknife sample, we use the invariance matrix of the entire ensemble, rather than recomputing the

Naik, $\beta_{\text{pl}} = 7.75, 16^3 \times 32$

am_q	π	π_2	ρ	ρ_2	Nucleon
0.01	0.26943(34)	0.5374(51)	0.829(18)	0.862(12)	1.140(80)
0.02	0.37638(30)	0.6175(42)	0.8951(96)	0.906(11)	1.265(26)
0.04	0.52339(20)	0.7421(22)	0.9701(47)	1.015(13)	1.429(10)
0.08	0.72718(18)	0.9428(14)	1.1071(22)	1.1479(77)	1.6855(35)
0.16	1.01186(16)	1.2587(17)	1.3577(65)	1.3963(26)	2.1018(42)

Kogut-Susskind, $\beta_{\text{pl}} = 7.75, 16^3 \times 32$

am_q	π	π_2	ρ	ρ_2	Nucleon
0.01	0.27794(33)	0.5445(50)	0.830(16)	0.863(11)	1.174(11)
0.02	0.38752(28)	0.6182(22)	0.8895(82)	0.8898(53)	1.282(10)
0.04	0.53656(21)	0.7504(21)	0.9632(41)	1.025(11)	1.4225(90)
0.08	0.73830(17)	0.9460(13)	1.0984(32)	1.1351(54)	1.6866(64)
0.16	1.00860(12)	1.2320(16)	1.3173(32)	1.3550(41)	2.0571(47)

Naik, $\beta_{\text{pl}} = 7.9, 16^3 \times 32$

am_q	π	π_2	ρ	ρ_2	Nucleon
0.005	0.18486(32)	0.3806(67)	0.6681(99)	0.6831(75)	0.920(12)
0.01	0.25907(28)	0.4284(48)	0.760(23)	0.725(11)	1.017(16)
0.02	0.36229(28)	0.5054(37)	0.7873(98)	0.7678(53)	1.0972(75)
0.04	0.50589(26)	0.6400(20)	0.8655(89)	0.8546(49)	1.2632(72)
0.08	0.70786(24)	0.8506(16)	1.0056(33)	1.0104(28)	1.5236(93)
0.16	0.99501(20)	1.1710(14)	1.2646(32)	1.2790(17)	1.9560(52)

Kogut-Susskind, $\beta_{\text{pl}} = 7.9, 16^3 \times 32$

am_q	π	π_2	ρ	ρ_2	Nucleon
0.005	0.19160(32)	0.3848(71)	0.6704(96)	0.6756(73)	0.9114(67)
0.01	0.26809(28)	0.4339(49)	0.720(24)	0.753(28)	1.005(15)
0.02	0.37383(31)	0.5142(36)	0.7767(87)	0.796(11)	1.0963(69)
0.04	0.51985(29)	0.6525(20)	0.8599(44)	0.8576(45)	1.2703(65)
0.08	0.72125(26)	0.8624(15)	1.0051(23)	1.0115(26)	1.5376(78)
0.16	0.99577(21)	1.1642(27)	1.2401(19)	1.2630(37)	1.9388(54)

Table 4: Masses for $\beta_{\text{pl}} = 7.75$ and $\beta_{\text{pl}} = 7.9, 16^3 \times 32$ lattices.

invariance matrix for each sample.

A generic feature of the fits to the propagators is that one has to use considerably larger minimum fit distance from the source with Naik fermions than with the Kogut-Susskind fermions. The reason for this effect is probably the large extent in the imaginary time

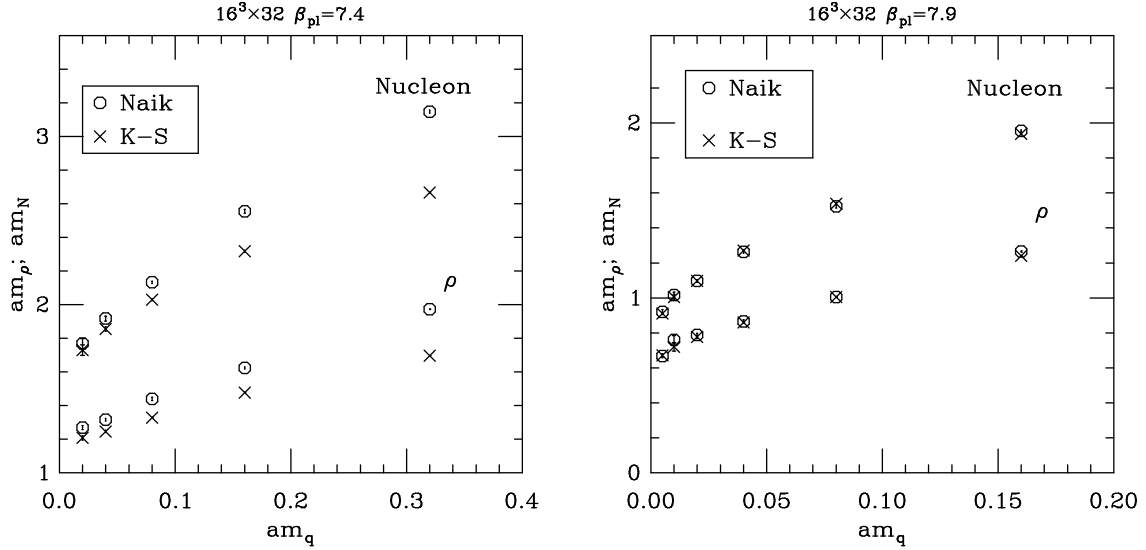


Figure 3: Nucleon (upper) and ρ (lower) masses as functions of am_q for $\beta_{\text{pl}} = 7.4$ and 7.9 .

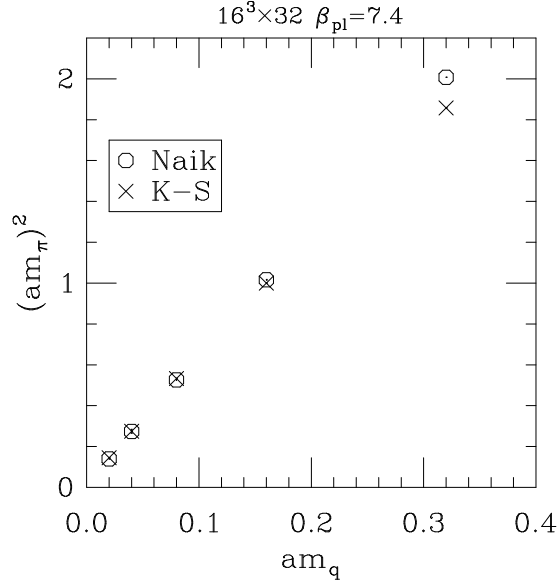


Figure 4: The pion mass squared as a function of am_q for $\beta_{\text{pl}} = 7.4$.

direction of the Naik derivative operator in Eq. (8) [19]. The transfer matrix is well defined only at imaginary time separations larger or equal to 3. The ghost branch in the dispersion relation can also cause short distance effects in the correlation function.

In Fig. 3 we summarise the nucleon and ρ meson masses from Tables 3 and 4 for $\beta_{\text{pl}} = 7.4$ and 7.9 , and in Fig. 4 the pion mass squared for $\beta_{\text{pl}} = 7.4$. The masses of the

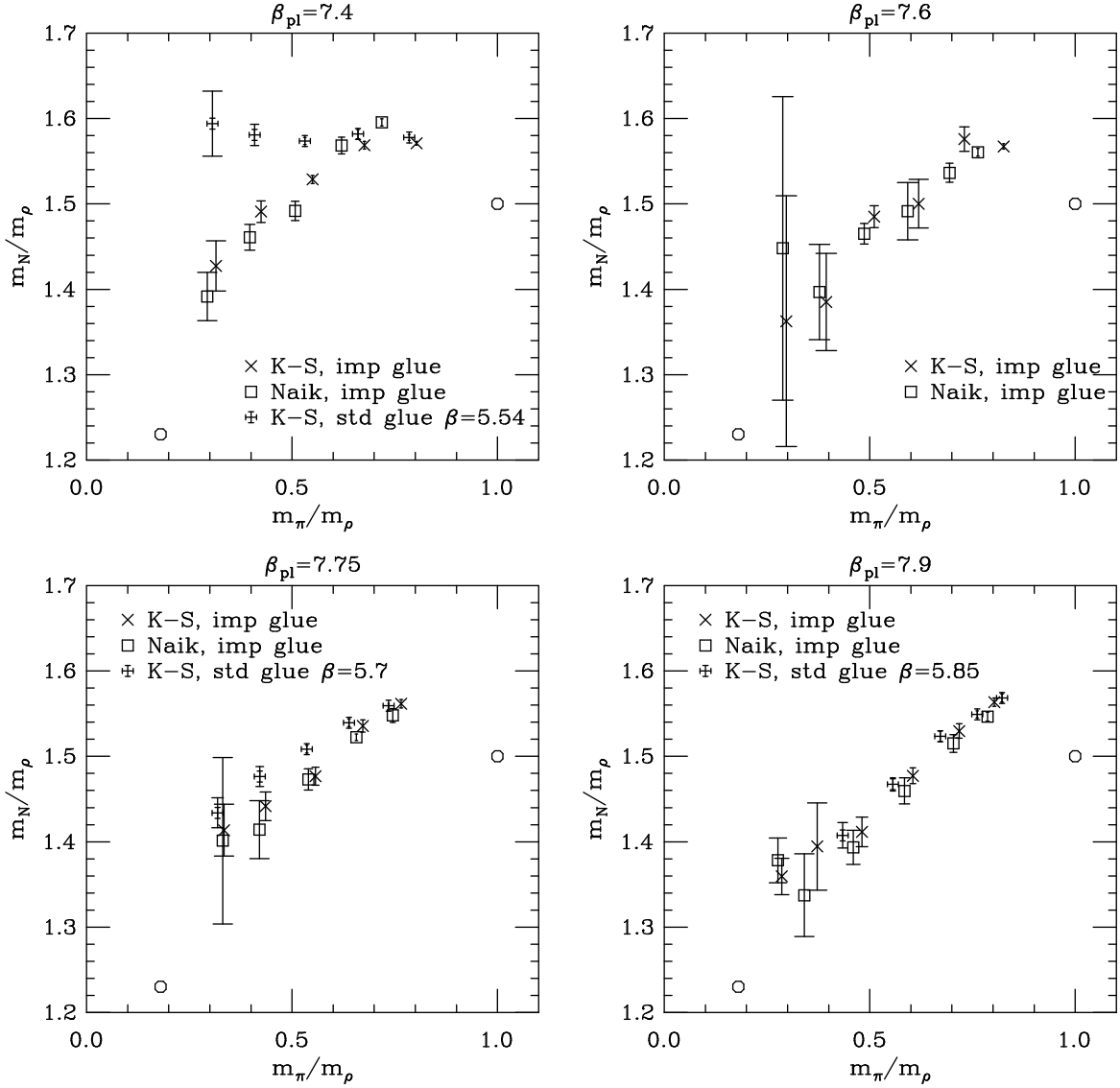


Figure 5: The Edinburgh plots for $\beta_{\text{pl}} = 7.4, 7.6, 7.75$ and 7.9 . The fancy crosses show the standard unimproved Kogut-Susskind data at $\beta_{\text{Wilson}} = 6/g^2 = 5.54, 5.7$ and 5.85 [11]; these correspond roughly to the same lattice spacing (determined by am_ρ) as the improved $\beta_{\text{pl}} = 7.4, 7.75$ and 7.9 . The small circles denote the physical limit ($m_\pi/m_\rho \approx 0.18$) and the infinite quark mass limit ($m_\pi/m_\rho = 1$).

Naik hadrons in lattice units tend to be larger than the Kogut-Susskind masses, but the difference gets smaller with decreasing am_q (approaching the chiral limit) and increasing β_{pl} (continuum limit). At $\beta_{\text{pl}} = 7.9$ the differences are barely discernible.

Figure 5 shows the Edinburgh plots for $\beta_{\text{pl}} = 7.4\text{--}7.9$. The m_N/m_ρ -ratios from $\beta_{\text{pl}} = 6.8$ and 7.1 exhibit typical strong coupling behavior: the ratio m_N/m_ρ remains roughly constant at around 1.5 when $m_q \rightarrow 0$ ($m_\pi/m_\rho \rightarrow 0$). Only when $\beta_{\text{pl}} \geq 7.4$ do the data show an approach to the vicinity of the physical value, and thus in the following we concentrate on these couplings. For comparison, we also plot the m_N/m_ρ mass ratio obtained with standard non-improved Kogut-Susskind action at $\beta = 5.54, 5.7$ and 5.85 [11]; these couplings correspond roughly to the same lattice spacing as the improved action at $\beta_{\text{pl}} = 7.4, 7.75$ and 7.9 .

It is interesting to note that despite the large differences in the masses in lattice units in Fig. 3 (and Table 3), in Fig. 5 the $\beta_{\text{pl}} = 7.4$ Naik and Kogut-Susskind mass ratios lie practically on the same curve, with the Naik values displaced slightly in the direction of smaller m_π/m_ρ . When the mass of the ρ meson is used to set the scale, from Figs. 3 and 5 we see that for a given set of bare parameters the lattice spacing for the Naik fermions is slightly larger than for the Kogut-Susskind fermions, while the mass ratios are closer to the physical values. Conversely, if we want to investigate the same *physical system* (mass ratio and physical volume), the Naik action enables us to use a bit larger bare quark mass and smaller lattices (in lattice units). This effect becomes smaller as one gets closer to the chiral limit $m_q \rightarrow 0$ and to the continuum limit $\beta_{\text{pl}} \rightarrow \infty$; nevertheless, it is clearly observable in all of the Edinburgh plots in Fig. 5.

3.2 The chiral function and the continuum limit

A convenient method to quantitatively measure the degree of improvement in hadron spectroscopy is to study the lattice spacing dependence (in units of am_ρ) of the ratio m_N/m_ρ at some fixed value of m_π/m_ρ . This requires interpolation or extrapolation to the desired m_π/m_ρ ratio. We perform this for each β_{pl} separately with chiral fit functions.

The chiral fits are motivated by quenched chiral perturbation theory ($Q\chi PT$), which gives m_N and m_ρ in a power series of m_π (+ logarithmic terms). Since in the leading order $m_\pi^2 \propto m_q$, these become power series in $m_q^{1/2}$. For the standard Kogut-Susskind action, the chiral extrapolations have been discussed in detail in [11].

Extrapolation of the ratio m_N/m_ρ to the chiral limit $m_\pi \rightarrow 0$ or even to the physical limit $m_\pi/m_\rho \approx 0.1753$ is sensitive to the form of the selected chiral fit function ansatz.

The value of the ratio is much less sensitive in the region $m_\pi/m_\rho \approx 0.4\text{--}0.6$, where the function interpolates between measured mass values (see Fig. 5). Detailed comparison of the different actions is feasible in this region.

We exclude the “strong coupling” runs at $\beta_{\text{pl}} = 6.8$ and 7.1 , and fit $am_N(am_q)$ and $am_\rho(am_q)$ for $\beta_{\text{pl}} = 7.4\text{--}7.9$ to the chiral ansatz

$$am = c_0 + c_1 am_q + c_{3/2}(am_q)^{3/2} + c_2(am_q)^2. \quad (15)$$

This function gives good fits at all 4 couplings (after excluding the anomalous smallest am_q value 0.005 from $\beta_{\text{pl}} = 7.9$).

Q χ PT for nucleons and vector mesons [20] implies the presence of an additional term $\propto am_\pi$, which corresponds to $(am_q)^{1/2}$ in the continuum. If one includes a term $\propto (am_q)^{1/2}$ in (15), the fits invariably prefer a positive sign for the coefficient; whereas Q χ PT gives a negative sign. However, the appropriate pion mass in this term is actually the flavor singlet pion mass, which is not proportional to $(am_q)^{1/2}$ at fixed lattice spacing due to flavor symmetry breaking. When this is taken into account, acceptable fits with a coefficient compatible both in sign and magnitude with Q χ PT are possible. This is studied in detail for our standard gauge Kogut-Susskind hadrons in Ref. [11]. Since such fits do not appear to change the extrapolated/interpolated values significantly from (15), but do increase the errors, we prefer to leave out the am_π term.

The error propagation is taken into account by performing the (fully correlated) fits separately to each of the jackknife blocks.

In most cases, it would be possible to obtain acceptable fits also with the simpler ansatz with either $c_{3/2}$ or c_2 fixed to zero. However, while the full ansatz (15) works quite well for the standard Kogut-Susskind hadrons [11], these simplified functions do not. In order to facilitate the comparisons between the different actions, we retain the full chiral ansatz (15) here.

The results of the chiral extrapolation/interpolation to $m_\pi/m_\rho = 0.1753$ (physical), 0.4, 0.5 and 0.7 are shown in Fig. 6; both for improved actions and for the standard Kogut-Susskind action. Since we expect the leading errors to be $\mathcal{O}(a^2)$, we plot the ratios against $(am_\rho)^2$. Here am_ρ is calculated at the quark mass which yields the indicated value of m_π/m_ρ . We make a linear fit with respect to $(am_\rho)^2$ of the standard Kogut-Susskind data, and, since in the continuum limit all of the actions must yield equivalent results,

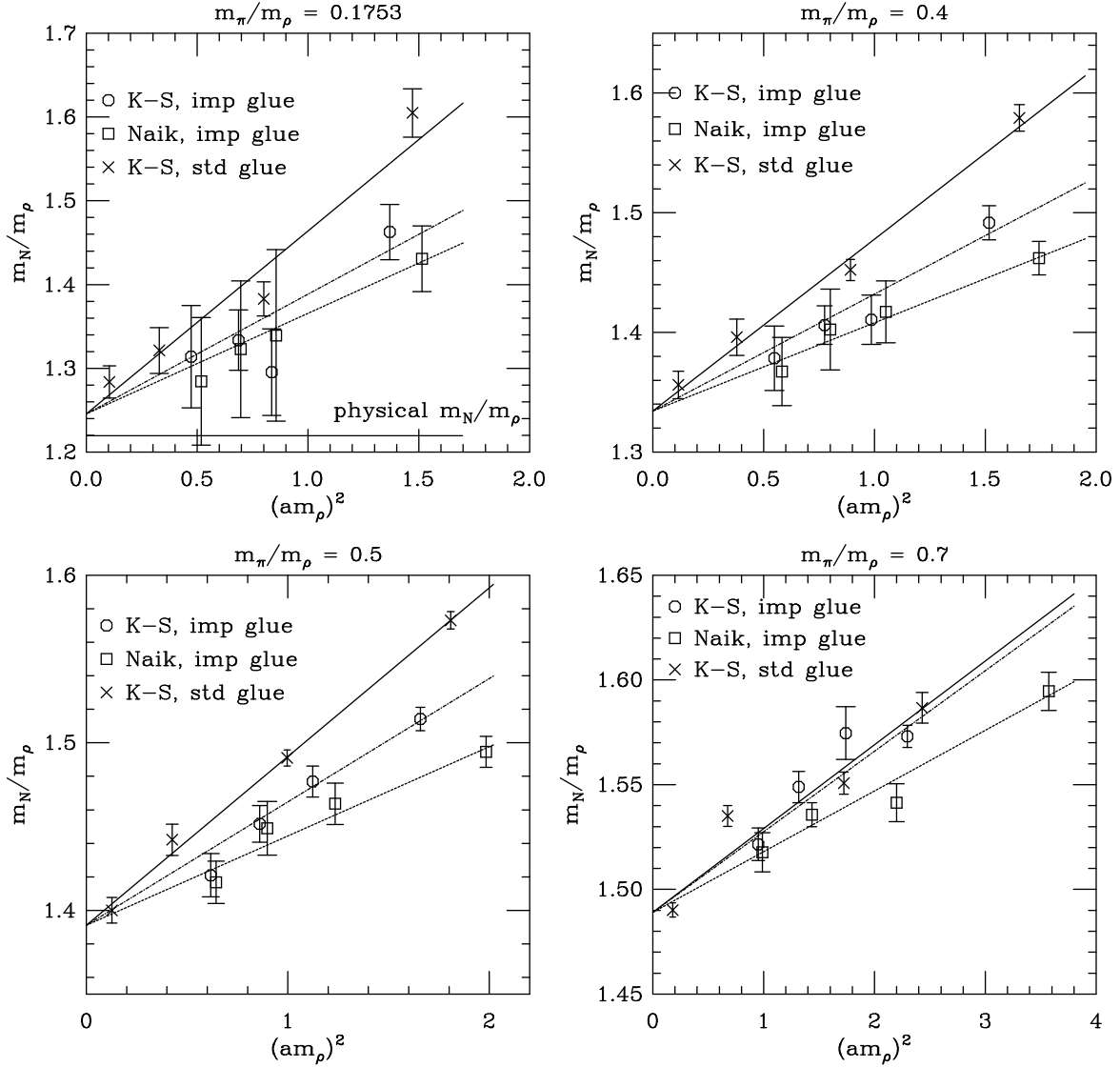


Figure 6: The m_N/m_ρ mass ratios as functions of the square of the lattice spacing (in units of $(am_\rho)^2$), for $m_\pi/m_\rho = 0.1753, 0.4, 0.5$ and 0.7 . From left to right, the Naik and the (improved gauge) Kogut-Susskind points correspond to $\beta_{\text{pl}} = 7.9, 7.75, 7.6$ and 7.4 ; the standard Kogut-Susskind points to $\beta_{\text{Wilson}} = 6.15, 5.85, 5.7$ and 5.54 . The straight lines are linear fits to the (from top to bottom) standard K-S, improved K-S and Naik data, where the intercept at $a = 0$ in the last two fits is fixed to the standard K-S value.

we fit straight lines to the improved Kogut-Susskind and Naik data, with the constraint that the $a = 0$ intercept is fixed to the standard Kogut-Susskind value.

We make the following observations:

- In the intermediate $m_\pi/m_\rho = 0.4$ and 0.5 plots, the improved gauge nucleon to ρ mass ratios are clearly closer to the continuum values than the standard Kogut-Susskind ones. Indeed, the $\beta_{\text{pl}} = 7.9$ value is very close to the standard Kogut-Susskind $\beta_{\text{Wilson}} = 6.15$ one, but with twice the lattice spacing (albeit with larger statistical errors). At large lattice spacings ($\beta_{\text{pl}} = 7.4$) the Naik fermions show smaller scaling violation than the improved gauge Kogut-Susskind fermions, but this difference becomes very small when the lattice spacing is reduced.
- At the physical ratio $m_\pi/m_\rho = 0.1753$ the errors in m_N/m_ρ increase dramatically due to the extrapolation in am_q . Nevertheless, we observe a pattern similar to that at larger quark mass.
- When $m_\pi/m_\rho = 0.7$ the quark mass am_q becomes so large that the chiral expansion (15) does not converge well any more: the highest power terms have the largest magnitude. This leads to erratic jumping of the points in the last panel of Fig. 6. (note however the very small range of m_N/m_ρ covered by this plot).
- As the quark mass is lowered, the difference between the two types of quarks in the improved gluonic fields is reduced. Thus, at $m_\pi/m_\rho = 0.7$ most of the improvement of m_N/m_ρ is attributable to the Naik improvement, whereas near the physical quark mass, most of the improvement comes from the gluonic action. A large part of the Naik improvement is due to the larger (am_ρ) and hence a larger lattice spacing. If one uses the string tension to set the scale the difference between the Naik and the Kogut-Susskind actions becomes smaller.
- The linearity (against $(am_\rho)^2$) of the standard Kogut-Susskind m_N/m_ρ -ratio clearly supports the notion that the scaling violations behave as $\mathcal{O}(a^2)$. When $m_\pi/m_\rho \leq 0.5$, the constrained linear fits to the improved gauge Kogut-Susskind and Naik data have confidence levels better than 0.5, certainly quite compatible with $\mathcal{O}(a^2)$ leading scaling violations. The magnitude of the violations – the slope of the line – for the Naik data is only about 1/2 of the standard Kogut-Susskind value, whereas the improved gauge Kogut-Susskind has a slightly larger slope than Naik.
- We can also test whether the data would allow for $\mathcal{O}(a^3)$ scaling violations for the

Naik action. When $m_\pi/m_\rho = 0.5$ a constrained fit of form $A + B(am_\rho)^3$ (where again A is set to the $a = 0$ intercept of the standard Kogut-Susskind data) does *not* fit the Naik data well: the confidence level is only 0.15 (as opposed to 0.75 before). This disfavors the leading $\mathcal{O}(a^3)$ errors. For smaller m_π/m_ρ -ratios the statistical errors become larger and this analysis cannot distinguish the fits.

- To check consistency, we can relax the constraint at $a = 0$ and fit independent straight lines to all datasets. When $m_\pi/m_\rho \leq 0.5$ the intercepts at $a = 0$ are compatible for all cases, *i. e.*, within 1 standard deviation of each other.

The lattice spacing and the size of the system in physical units can be obtained by extrapolating am_ρ to the physical m_π/m_ρ -ratio and setting $m_\rho = 770$ MeV. These are given in Table 5.

β_{pl}	6.8	7.1	7.4	7.6	7.75	7.9
a (fm)	0.37	0.35	0.31	0.24	0.21	0.19
Size (fm)	5.9	5.0	5.0	3.8	3.4	3.0

Table 5: The lattice spacing and the box size in physical units.

The numbers in Table 5 have been calculated with the Naik quark action; for the Kogut-Susskind action the lattice spacings and the box sizes would be fractionally smaller. The box sizes are considerably larger than 2 fm (with the possible exception of $\beta_{\text{pl}} = 7.9$), so that we can safely ignore the finite size effects [21]. For the weakest coupling and the smallest quark mass, the product $m_\pi \times (\text{Lattice size})$ is approximately 3.0.

Besides the mass of the ρ -meson, the square root of the string tension is commonly used to determine the lattice spacing. In Fig. 7 the ratio $m_\rho/\sqrt{\sigma}$ is plotted against $a^2\sigma$. Here am_ρ is evaluated at the physical $m_\pi/m_\rho = 0.1753$ and at 0.7. The string tension for the standard gauge action is interpolated from the data in the literature [22]; for the improved gauge action (1) it has been measured by the SCRI group [23].

Since the scale violations are expected to behave as $\mathcal{O}(a^2)$, the $m_\rho/\sqrt{\sigma}$ ratio should behave linearly as a function of $a^2\sigma$. Indeed, the standard Kogut-Susskind data shows good linearity up to $a^2\sigma = 0.17$ ($\beta_{\text{Wilson}} = 5.7$). However, at stronger coupling (5.54) the ratio falls strongly off the linear behavior. We fit a straight line to the three weakest coupling datapoints, the intercepts at $a = 0$ are 1.738(25) at the physical $m_\pi/m_\rho =$

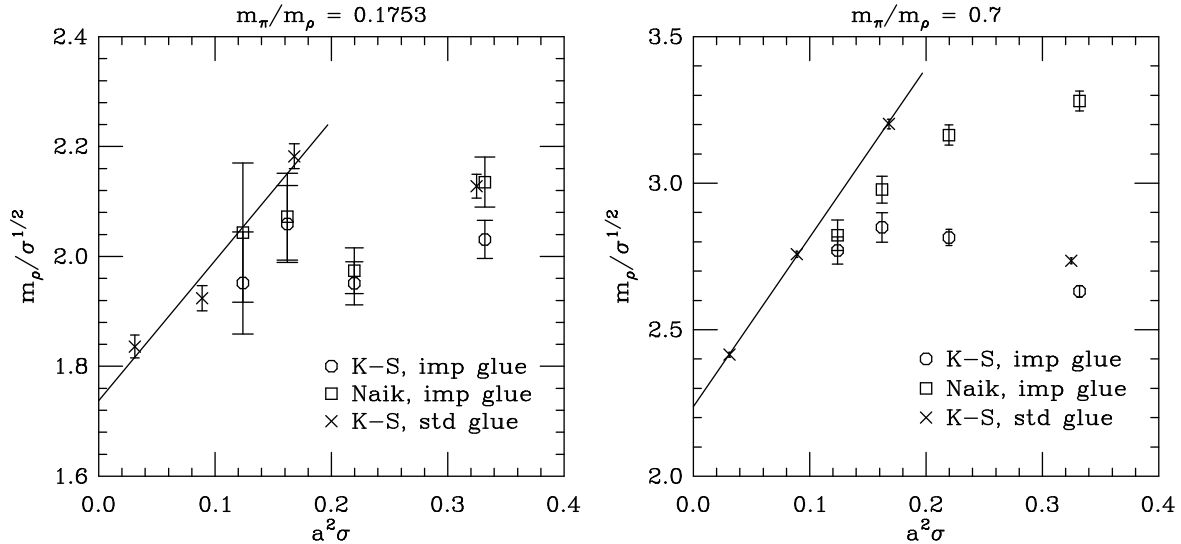


Figure 7: The ratio $m_\rho/\sqrt{\sigma}$ against $a^2\sigma$ at $m_\pi/m_\rho = 0.1753$ and 0.7 .

0.1753 and 2.238(11) at 0.7 (the errors quoted here are only statistical). These results are consistent with the SCRI group (preliminary) Wilson and clover fermion mass ratios [23].

The improved gauge Kogut-Susskind and Naik data still seem to reside completely in the “strong coupling region”, although there is some indication that at weaker couplings the ratios would bend to the direction of the line defined by the standard Kogut-Susskind data. Extrapolation of the improved action ratios to the continuum limit is clearly not justified.

The non-linearity in $m_\rho/\sqrt{\sigma}$ is somewhat surprising, when we compare it against the purely hadronic observables in Fig. 6. This lends support to the view that a large part of the scaling violations cancel in the hadronic ratios, and justifies the use of am_ρ as the scale factor in purely hadronic observables.

3.3 Lorentz symmetry

As discussed in Sec. 2.3, the free quark continuum dispersion relation is approximated much better by the Naik action than by the standard Kogut-Susskind action. At very high temperatures, deep in the quark-gluon plasma phase, the quarks behave approximately as free particles, and the Naik action improves QCD thermodynamics [10]. However, *a priori* it is not clear whether the dispersion relation of hadronic states is improved.

	Kogut-Susskind π		Naik π	
$\mathbf{k}L/(2\pi)$	$aE(\mathbf{k})$	$c^2(\mathbf{k})$	$aE(\mathbf{k})$	$c^2(\mathbf{k})$
(0,0,0)	0.53521(17)	-	0.52625(15)	-
(0,0,1)	0.65223(56)	0.9010(45)	0.65111(50)	0.9532(39)
(0,1,1)	0.74710(63)	0.8809(30)	0.75474(76)	0.9489(36)
(1,1,1)	0.82655(88)	0.8575(31)	0.8411(11)	0.9305(40)
(0,0,2)	0.8817(14)	0.7959(40)	0.9087(26)	0.8897(77)
(0,2,2)	1.0925(32)	0.7353(57)	1.1549(44)	0.8566(83)
(2,2,2)	1.275(11)	0.723(15)	1.395(19)	0.902(29)

	Kogut-Susskind ρ		Naik ρ	
$\mathbf{k}L/(2\pi)$	$aE(\mathbf{k})$	$c^2(\mathbf{k})$	$aE(\mathbf{k})$	$c^2(\mathbf{k})$
(0,0,0)	1.2411(69)	-	1.3065(79)	-
(0,0,1)	1.262(27)	0.34(44)	1.3489(80)	0.73(15)
(0,1,0)	1.289(13)	0.79(21)	1.362(16)	0.97(28)
(0,1,1)	1.298(13)	0.47(11)	1.385(19)	0.68(16)
(1,1,0)	1.320(18)	0.65(16)	1.385(12)	0.68(12)

Table 6: The energy of the π and ρ meson states at finite momentum $\mathbf{k} = \mathbf{n}2\pi/L$, and the ‘speed of light squared’ $c^2(\mathbf{k}) = (E^2(\mathbf{k}) - E^2(0))/\mathbf{k}^2$, for $\beta_{\text{pl}} = 7.4$, $am_q = 0.04$, $16^3 \times 32$ lattice.

We test hadron dispersion relations by measuring the energy of the π - and ρ -meson states with finite spatial momenta on 100 lattices with $\beta_{\text{pl}} = 7.4$, $am_q = 0.04$ and volume $16^3 \times 32$. We use 4 (finite momentum) wall sources, separated by 8 lattice units.

The source operators are constructed as follows: first, we take a zero momentum wall source, which is 1 for a particular source color at each spatial slice at the source time. This is used as a source for the conjugate gradient to compute the quark propagators. Then this wall source is multiplied by the momentum dependent phase factor $\exp(i\mathbf{k} \cdot \mathbf{x})$, by the sign factors (depending on the location in the 2^4 flavor hypercube) to select the desired meson, and by an extra $(-1)^{\sum_\mu x_\mu}$ corresponding to γ_5 . This is used as a source for the conjugate gradient to compute the antiquark propagator. The sink operator is similar, except that the quark and antiquark propagators are multiplied together with the appropriate phase and sign factors before summing over spatial points, corresponding to a local sink.

For pions, we use momentum vectors pointing to 3 different directions: $\mathbf{k}L/(2\pi) = (0, 0, 1)$, $(0, 1, 1)$, $(1, 1, 1)$, and these multiplied by 2. For the ρ -meson, we use (the lattice

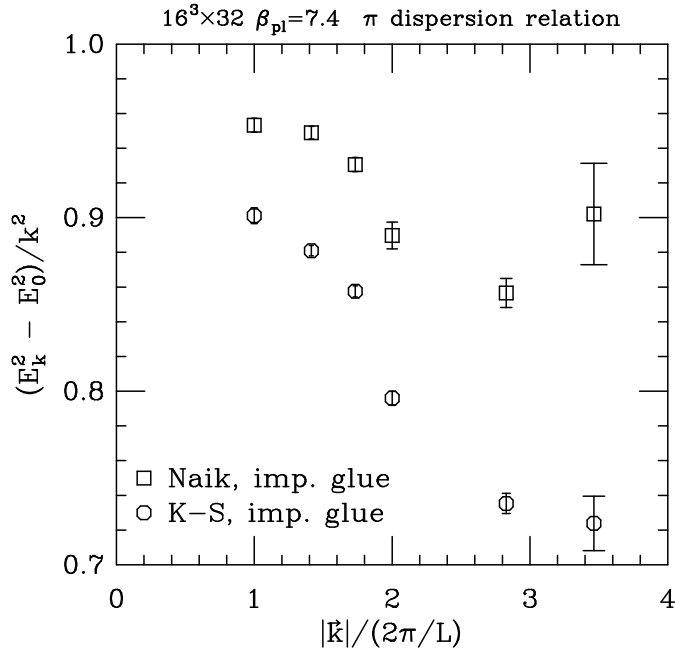


Figure 8: The ‘speed of light squared’, calculated from the pion dispersion relation, for Naik and K-S pions.

analog of) the vector operator $\bar{\psi}\gamma_3\psi$, and we expect that the dispersion relation may be different along the z -axis direction and perpendicular to it. Therefore, for ρ we use $\mathbf{k}L/(2\pi) = (0, 0, 1)$, $(0, 1, 0)$, $(0, 1, 1)$ and $(1, 1, 0)$. The signals for higher momenta are too noisy to be useful. The results are listed in Table 6.

The violation of Lorentz invariance can be quantified by measuring the ‘speed of light’ with the continuum dispersion relation

$$c^2(\mathbf{k}) = \frac{E^2(\mathbf{k}) - E^2(0)}{\mathbf{k}^2}. \quad (16)$$

The deviation of c^2 from unity directly measures the violation of Lorentz invariance. The results are shown in Table 6 and in Fig. 8 (for pions). The Naik pions show a clear improvement of c^2 over the Kogut-Susskind pions: the deviation from unity is reduced approximately by half. The results for the ρ -mesons seem to indicate a dependence on the direction of the momentum (parallel or perpendicular to z). Also, here the c^2 is closer to unity for the Naik mesons; however, the statistical errors are so large that we cannot make definite statements about the improvement.

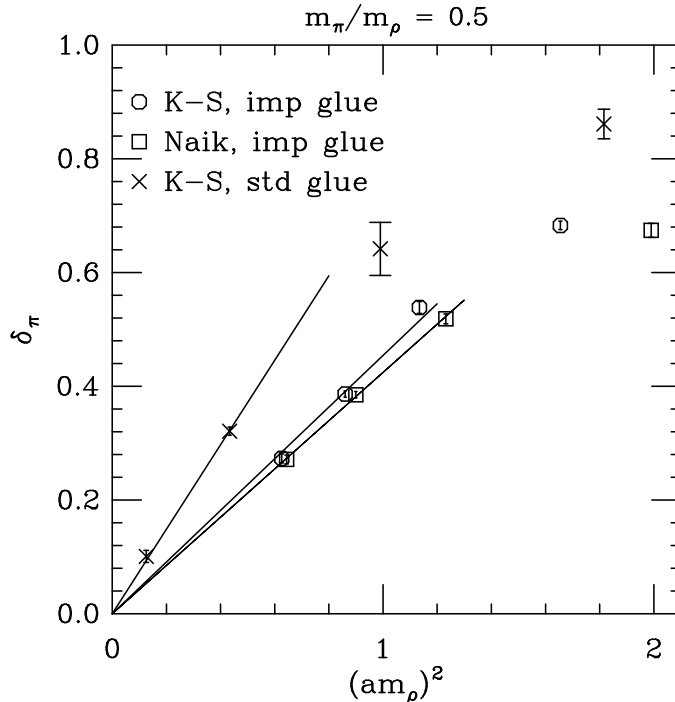


Figure 9: Flavor symmetry breaking parameter $\delta_\pi = (m_{\pi_2}^2 - m_\pi^2)/(m_\rho^2 - m_\pi^2)$, interpolated to $m_\pi/m_\rho = 0.5$, as a function of $(am_\rho)^2$. The data correspond to the same values of β as in Fig. 6. The straight lines are linear fits to 2 (standard gauge) or 3 (improved gauge) points with the smallest lattice spacings, constrained to go through the origin.

3.4 Flavor symmetry

The restoration of flavor symmetry can be discerned by investigating the mass differences between π and π_2 mesons. The first particle is the Goldstone boson corresponding to the spontaneously broken $U(1) \times U(1)$ chiral symmetry and it becomes massless when $am_q \rightarrow 0$ even at a finite lattice spacing (Fig. 4). In comparison, the π_2 mesons remain massive in the chiral limit, and become massless only when both the chiral and the continuum limits are taken.

We use the dimensionless quantity

$$\delta_\pi = \frac{m_{\pi_2}^2 - m_\pi^2}{m_\rho^2 - m_\pi^2} \quad (17)$$

to measure flavor symmetry breaking. For the standard Kogut-Susskind quark action, this quantity is almost independent of the bare quark mass am_q at small lattice spacings. In Fig. 9, we show δ_π for $\beta_{pl} \geq 7.4$ improved gauge Naik and Kogut-Susskind hadrons,

together with the unimproved glue Kogut-Susskind values, as functions of $(am_\rho)^2$. The data is interpolated to $m_\pi/m_\rho = 0.5$ (compare to the third panel in Fig. 6). With this constraint, the flavor symmetry breaking parameter reduces to $\delta_\pi = (m_{\pi 2}^2/m_\pi^2 - 1)/3$.

At this value of m_π/m_ρ , we observe that the flavor symmetry violation at small a is reduced by $\approx 45\%$ due to the improved gauge action. When the Naik fermions are used, δ_π is slightly smaller than with the Kogut-Susskind fermions. However, this situation would become reversed, if we used $a\sqrt{\sigma}$ instead of am_ρ to set the scale.

Figure 9 clearly indicates that the leading flavor symmetry breaking terms are proportional to a^2 for all of the actions studied. The region linear in $(am_\rho)^2$ extends to larger lattice spacings with the improved gauge.

A successful additional improvement of the Kogut-Susskind flavor symmetry is the MILC “fat link” fermion action [9]. That action substitutes the standard gauge links with smeared average links in the fermion hopping terms. The averaging process improves the flavor symmetry dramatically, the improvement being roughly comparable both for the standard Kogut-Susskind and the Naik action. These observations indicate the importance of the coupling of fermions to the gauge fields for the flavor symmetry of the staggered action. The Naik action (8) can be interpreted naively as a straightforward improvement of the (free) fermion dispersion relation.

The improvement in flavor symmetry from the Symanzik improved gauge action, like the improvement from the fat link quark action, can be understood as a suppression of the effects of high momentum gluons. Gluons with momentum near π/a scatter quarks from one corner of the Brillouin zone to another, which is roughly equivalent to changing their flavor [24, 25]. The suppression of the high momentum gluons becomes evident when the gauge action is expanded to quadratic order in the vector potential A_μ (where the lattice variable $U_\mu(x) = \exp[-igaA_\mu(x)]$). Using the shorthand notations

$$\hat{k}_\mu = 2 \sin \frac{1}{2} ak_\mu, \quad \hat{k}^2 = \sum_\mu \hat{k}_\mu^2, \quad (18)$$

and

$$f_{\mu,\nu}(k) = \hat{k}_\mu A_\nu(k) - \hat{k}_\nu A_\mu(k), \quad (19)$$

the quadratic part of the action (1) can be written in the form [26]

$$S^{(2)} = \frac{1}{2} a^2 \sum_{k;\mu<\nu} f_{\mu,\nu}(k) f_{\mu,\nu}(-k) \left[c_{\text{pl}} + 8c_{\text{rt}} + 16c_{\text{pg}} - (c_{\text{rt}} - c_{\text{pg}})(\hat{k}_\mu^2 + \hat{k}_\nu^2) - c_{\text{pg}}\hat{k}^2 \right]. \quad (20)$$

Here the coefficients c_i denote the relative strength of the three terms in the action. They are related to coefficients β_i through $c_i 6/g^2 = \beta_i$. As an overall normalization we require that the constant term within the brackets equals to one: $c_{\text{pl}} + 8c_{\text{rt}} + 16c_{\text{pg}} = 1$.

For the Wilson gauge action the coefficients are $c_{\text{pl}} = 1$, $c_{\text{rt}} = c_{\text{pg}} = 0$, whereas for the improved action $c_{\text{pl}} > 1$ and $c_{\text{rt}}, c_{\text{pg}} < 0$. With the improved gauge, the non-constant terms within the brackets in Eq. (20) increase the action for modes close to the edges of the Brillouin zone ($k_\mu \approx \pm\pi/a$, for at least one μ).

As a simple example we consider a momentum vector parallel to one of the lattice axes and at the edge of the zone. In this case the term within the brackets in Eq. (20) reduces to $[1 - 4c_{\text{rt}}]$. At $\beta_{\text{pl}} = 7.4$, using Eqs. (5,6), Table 1 and the normalization condition above, the coefficient c_{rt} has a value ≈ -0.26 . When compared to the Wilson gauge action ($c_{\text{rt}} = 0$), this more than doubles the action difference of the modes close to the edge of the zone and near the origin $k = 0$. When the lattice spacing is reduced the suppression of the modes near the edge of the zone increases rapidly, while the relative difference between the actions becomes smaller. At tree level, the coefficients assume values $c_{\text{pl}} = 5/3$, $c_{\text{rt}} = -1/12$ and $c_{\text{pg}} = 0$, still yielding a 33% difference of the action at $k_\mu = \pi/a$.

4 Conclusions

We investigate improvement of the quenched light hadron mass spectrum using a tadpole-improved staggered Naik action (8), which at the tree level does not have $\mathcal{O}(a^2)$ errors. Correspondingly, we use $\mathcal{O}(a^2)$ tadpole improved gauge action to generate the gauge configurations. Using the same gauge action for both the Kogut-Susskind and the Naik calculations allows us to separate the effect of the fermionic improvement from the improvement of the gauge action. The latter is studied by comparing the results presented here to our standard Kogut-Susskind results [11].

We find that improvement of the gauge action has a significant effect on the hadron spectrum: when $m_\pi/m_\rho \sim 0.5$, the nucleon to ρ -meson mass ratio is roughly 50% closer to the continuum value with the improved gauge than with the standard gauge action. Thus, the scale violations with the standard gauge spectroscopy are at roughly the same level as with the improved gauge at about 1.4 times the lattice spacing. Using the improved

gauge action, the Naik quark action has smaller scaling violations than the Kogut-Susskind action, although the difference becomes small when the quark mass is reduced. Similarly, improving the gauge action reduces the amount of flavor symmetry breaking, but using the Naik action yields little further gains. For both of the actions the flavor symmetry can be further improved with the ‘fat link’ procedure [9].

The biggest improvement provided by the Naik action comes from the improved Lorentz invariance of the hadronic states. This is best evidenced by the π -meson dispersion relation, which is much closer to the continuum behavior when the Naik action is used. This property may be especially significant for nonzero temperature simulations, where the hadronic and/or quark degrees of freedom typically have large momenta. Thus, when one strives for higher precision in staggered quark simulations, an economical solution can be found from the combination of an improved Naik-like quark action together with the fat links.

Acknowledgements

Discussions with E. Laermann are gratefully acknowledged. This work was supported by the U.S. Department of Energy under grants DE-AC02-76CH-0016, DE-AC02-86ER-40253, DE-FG02-91ER-40661, DE-FG02-91ER-40628, DE-FG03-95ER-40894, DE-FG03-95ER-40906, DE-FG05-85ER250000, DE-FG05-96ER-40979, and National Science Foundation grants NSF-PHY96-01227 and NSF-PHY97-22022. The computations have been performed on the Intel Paragon at Indiana University, on the DEC Alpha server and Cray T3E at the Pittsburgh Supercomputing Center, on the Intel Paragon and Cray T3E at the San Diego Supercomputing Center, and on the CM-2 at SCRI.

References

- [1] K. Symanzik, in “Recent Developments in Gauge Theories”, eds. G. ’t Hooft et al. 313 (Plenum, New York, 1980); Nucl. Phys. **B226** 187 (1983).
- [2] M. Lüscher and P. Weisz, Comm. Math. Phys. **97** 19 (1985); Phys. Lett. **158B** 250 (1985).
- [3] G. P. Lepage and P. B. Mackenzie, Phys. Rev. **D48** 2250 (1993) [[hep-lat/9209022](#)].

- [4] T. DeGrand, A. Hasenfratz, P. Hasenfratz and F. Niedermayer, Nucl. Phys. **B454** 587 (1995) [[hep-lat/9506030](#)]; Nucl. Phys. **B454** 615 (1995) [[hep-lat/9506031](#)].
- [5] W. Bietenholz and U.-J. Wiese, Nucl. Phys. **B** (Proc. Suppl.) **34** (1994) 516 [[hep-lat/9311016](#)]; H. Dilger, Nucl. Phys. **B490** (1997) 331 [[hep-lat/9610029](#)]; W. Bietenholz, R. Brower, S. Chandrasekharan and U.-J. Wiese, Nucl. Phys. **B495** (1997) 285 [[hep-lat/9612007](#)].
- [6] F. Niedermayer, review in the proceedings of “Lattice ’96”, Nucl. Phys. **B** (1997) **53** 56 (1997) [[hep-lat/9608097](#)].
- [7] S. Naik, Nucl. Phys. **B316** 238 (1989).
- [8] C. Bernard et al. (MILC collaboration), Nucl. Phys. **B** (Proc. Suppl.) **53** 212 (1997) [[hep-lat/9608102](#)];
to appear in the proceedings of “Lattice ’97”, Nucl. Phys. **B** (Proc. Suppl.) [[hep-lat/9711013](#)].
- [9] T. Blum, C. DeTar, S. Gottlieb, K. Rummukainen, U.M. Heller, J. Hetrick, D. Toussaint, R.L. Sugar, M. Wingate Phys. Rev. **D55** 1133 (1997) [[hep-lat/9609036](#)].
- [10] F. Karsch, B. Beinlich, J. Engels, R. Joswig, E. Laermann, A. Peikert and B. Petersson, Nucl. Phys. **B** (Proc. Suppl.) **53** 413 (1997) [[hep-lat/9608047](#)].
- [11] C. Bernard et al. (MILC collaboration), to appear in the proceedings of the workshop “Lattice QCD on Parallel Computers”, (Tsukuba 1997), IUHET-366 [[hep-lat/9707014](#)]; full report in *Continuum Limit of Lattice QCD with Staggered Quarks in the Valence Approximation — A Critical Role for the Chiral Extrapolation*, in preparation.
- [12] M. Alford, W. Dimm, G.P. Lepage, G. Hockney and P.B. Mackenzie, Phys. Lett. **B361** 87 (1995) [[hep-lat/9507010](#)].
- [13] H.S. Sharatchandra, H.J. Thun, P. Weisz Nucl. Phys. **B192** 205 (1981); M.F.L. Golterman and J. Smit, Nucl. Phys. **B245** 64 (1984).

- [14] H. Kluberg-Stern, A. Morel, O. Napoly, B. Petersson, Nucl. Phys. **B220** [FS8] 447 (1983).
- [15] S. Sharpe, Nucl. Phys. **B** (Proc. Suppl.) 34 403 (1994) [[hep-lat/9312067](#)].
- [16] Y. Luo, Phys. Rev. **D 55** 353 (1997) [[hep-lat/9604025](#)].
- [17] Y. Luo, Columbia University preprint CU-TP-186 [[hep-lat/9702013](#)].
- [18] F. Karsch, to appear in the proceedings of the workshop “Lattice QCD on Parallel Computers”, (Tsukuba 1997) [[hep-lat/9706006](#)]; A. Peikert, B. Beinlich, A. Bicker, F. Karsch and E. Laermann, to appear in Nucl. Phys. B(Proc. Suppl.) [[hep-lat/9709157](#)].
- [19] M. Lüscher and P. Weisz, Nucl. Phys. **B240** 349 (1984).
- [20] J. Labrenz, S. Sharpe, Phys. Rev. **D54** 4595 (1996) [[hep-lat/9605034](#)]; M. Booth, G. Chiladze and A. Falk, Phys. Rev. **D55** 3092 (1997) [[hep-ph/9610532](#)].
- [21] S. Gottlieb, Nucl. Phys. **B** (Proc. Suppl.) **53** 155 (1997) [[hep-lat/9608107](#)].
- [22] G. Bali and K. Schilling, Phys. Rev. **D46** 2636 (1992); G. Boyd, J. Engels, F. Karsch, E. Laermann, C. Legeland, M. Lütgemeier and B. Petersson, Nucl. Phys. **B469** 419 (1996) [[hep-lat/9602007](#)]; R.G. Edwards, U.M. Heller and T.R. Klassen, Florida State University preprint FSU-SCRI-97-122 [[hep-lat/9711033](#)].
- [23] S. Collins, R.G. Edwards, U.M. Heller and J. Sloan, in proceedings of the International Conference “Multiscale Phenomena and Their Simulation”, Bielefeld, Germany 1996, eds. F. Karsch, B. Monien and H. Satz, World Scientific (1997) [[hep-lat/9611022](#)].
- [24] P. Lepage, to appear in proceedings of the workshop “Lattice QCD on Parallel computers” (Tsukuba, 1997) [[hep-lat/9707026](#)].
- [25] J.F. Lagaë and D.K. Sinclair, to appear in the proceedings of “Lattice ’97”, Nucl. Phys. **B** (Proc. Suppl.) [[hep-lat/9709035](#)].
- [26] P. Weisz, Nucl. Phys. **B212** 1 (1983).